ELSEVIER

Engineering Analysis with Boundary Elements 30 (2006) 687–696

ENGINEERING ANALYSIS with BOUNDARY ELEMENTS

www.elsevier.com/locate/enganabound

Computation of 3D MEMS electrostatics using a nearly exact BEM solver

S. Muhkopadhyay*, N. Majumdar

Saha Institute of Nuclear Physics, 1/AF, Sector 1, Bidhannagar, Kolkata 700064, West Bengal, India

Received 11 August 2005; accepted 10 March 2006
Available online 15 May 2006

Abstract

The electrostatic properties of thin plate shaped structures relevant to the micro-electro-mechanical systems (MEMS) have been computed using a nearly exact boundary element method (BEM) solver. The solver uses closed form expressions for three-dimensional potential and force fields due to uniform sources/sinks distributed on finite flat surfaces. The expressions have been validated and, being analytical, have been found to be applicable throughout the physical domain. The solver has been applied to compute accurately and efficiently the charge densities on thin plate shaped conductors as used in MEMS components. We have presented results for the model problem of parallel plate capacitors and compared them with results obtained from several other BEM based solvers.

Keywords: Boundary element method; Green function; Electrostatics; MEMS; Thin plates

1. Introduction

The boundary element method (BEM) has been successfully applied to various branches of science and technology including gravitation, fluid mechanics, acoustics, structural mechanics, electronics and micro-electro-mechanical systems (MEMS). The method can be viewed as the numerical implementation of boundary integral equations (BIEs) based on the Green's formula. In order to carry out the implementation, only the boundaries need to be segmented. The resulting boundary elements are endowed with distribution of singularities such as sources, doublets, dipoles and vortices. The strength of these singularities are obtained by satisfying the boundary conditions (Dirichlet, Neumann or Robin). Thus, in comparison to finite element method (FEM) and finite difference method (FDM), numerical discretization for BEM is carried out at a reduced spatial dimension and the resulting linear system of equations are smaller. Moreover, due to the nature of Green's formula, the method works accurately for problems with unbounded domains without invoking truncation and other approximations necessary for FEM and FDM. There are several other advantages of using the BEM, e.g., mesh adjustment for moving boundaries is easier to carry out, no interpolation/extrapolation is required for obtaining properties at an arbitrary point in the domain. There are some disadvantages associated with the method as well. For example, the mathematics related to the formulation of a BEM solver is considerably more complex than that for FDM and FEM solvers. Moreover, the matrices generated through this formulation are fully populated and difficult to both generate and solve [1,2]. The most serious drawbacks, however, are related to the approximations involved in the numerical implementation of the BEM. They are, in general, as follows:

- While computing the influences of the singularities, the singularities are modeled by a sum of known basis functions with constant unknown coefficients. For example, in the constant element approach, the singularities are assumed to be concentrated at the centroid of the element, except for special cases such as self influence. This becomes necessary because closed form expressions for the influences are not, in general, available for surface elements. An approximate and

*Corresponding author. Fax: +91 33 23374637.
E-mail address: supratik.mukhopadhyay@saha.ac.in (S. Muhkopadhyay).

0955-7997/$ - see front matter © 2006 Elsevier Ltd. All rights reserved.
doi:10.1016/j.enganabound.2006.03.002

computationally rather expensive way of circumventing this limitation is to use numerical integration over each element or to use linear or higher order basis functions.
- The strengths of the singularities are solved depending upon the boundary conditions, which, in turn, are modeled by the shape functions. For example, in the constant element approach, it is assumed that it is sufficient to satisfy the boundary conditions at the centroids of the elements. In this approach, the position of the singularity and the point where the boundary condition is satisfied for a given element usually matches and is called the collocation point.

It may be noted here that the majority of implementations based on BEM are still the constant collocation approaches. This is because the method is a good optimization between accuracy and computational complexity. Both these approximations, especially the former, have important consequences. It leads to the unhappy situation where the potential and force field very close to the element are found to suffer from gross inaccuracies. So much so that a number of workers have had to devise ways of dealing with special cases through which the errors can be reduced to an acceptable extent [3–6]. However, these special formulations are not valid for the entire physical domain and thus, necessitate the use of several expressions for evaluating potential and field on the charged surfaces and other field points. It also becomes necessary to subdivide the segments on some parts of the boundary to justify certain approximations used to deduce the expressions.

Accuracy of the near-field calculations becomes exceedingly important for the structures used in MEMS which normally have fixed or moving structures with thickness (h) of the order of microns (μm) and lengths (L) of the order of tens or hundreds of microns. These structures are often plates or array of thin beams which, owing to their smallness, can be moved or deflected easily through the application of low voltages and are widely used in microjets, microspeakers, electrostatic actuators etc. Since electrostatic forces play a very major role in maneuvering these devices, a thorough understanding of the electrostatic properties of these structures is of critical importance, especially in the design phase of MEMS. In many cases, the electrostatic analysis of MEMS is carried out using BEM, while the structural analysis is carried out using FEM [7]. In this paper, we concentrate on the computation of the electrostatic properties (e.g., the charge distribution and the capacitance) of thin plates relevant to MEMS using BEM.

It has already been noted [6] that computing the resultant charge due to the two surfaces of a plate under the usual assumption of vanishing thickness of the plate is not an acceptable approach for these structures. This is so because the electrostatic force acting at any point on these surfaces depends on the square of the charge density at that point. The two surfaces of the plate being too near, the standard BEM does not work satisfactorily and several modified BEM have been developed, such as the enhanced BEM and the gradient BIE technique leading to the thin plate BEM [6]. The former is suitable for moderately thick plates, while the latter is suitable for very thin plates, $h/L \leqslant 10^{-3}$.

In this work, we present a BEM solver which overcomes the first approximation mentioned earlier by using closed-form expressions for computing influences that are valid for sources distributed uniformly over a flat surface. As a result, the first (and possibly, the most damaging) approximation for this solver can be relaxed and restated as,

- The singularities distributed on the boundary elements are assumed to be uniform on a particular element. The strength of the singularity may change from element to element.

Thus, our approximation turns to be far less stringent than the necessity to assume the singularity to be concentrated at one single point on an element. This relaxation has profound consequences for the solver and to reflect this fact, we have named the new solver a nearly exact BEM solver. Since the expressions used in this solver are analytic and valid for the complete physical domain, and no approximations regarding the size or shape of the singular surface have been made during their derivation, its application is not limited by the proximity of other singular surfaces or their curvature. In other words, it is possible to apply the solver for solving a very wide range of problems including those containing extremely closely spaced singular surfaces of any shape and size which are known to create major problems for other approaches developed and used so far. Thus, now, the same solver can be easily applied to compute properties for plates of any thickness and applicable for any structure, including those relevant to MEMS, for which electrostatic properties need to be computed. The necessity for special formulations to tackle the near-field domain does not arise at all. The approach, naturally, is not limited to electrostatics only but can be applied to many other fields of science and engineering where similar formulations are obtained.

In Section 2, we have presented a brief discussion on the theory of BEM and the new analytic expressions for the potential and the force field for a flat element having source uniformly distributed on it. In Section 3, we present the numerical implementation of the BEM solver, especially in the context of the MEMS thin plates. The first part of Section 4 contains the validation of the new expressions. Here we also study the effect of using the new expressions vis a vis implementing the usual BEM approximation. In the second part, we present the computation related to plates for a wide range of h/L and d/L where d is the distance between the facing sides of the two plates of a parallel plate capacitor. Here, as in [6], we concentrate on the charge density and the capacitance of the structures,

both of which are known to be very important for the design of efficient MEMS. We have compared our results with some of those available in the literature and, in some cases, our results seem to be better than the available ones. Finally, in Section 5, we present our conclusions.

2. Theory

The Laplace and the Poisson equations are two very widely used partial differential equations which occur in various branches of science and engineering such as gravitation, ideal fluid mechanics, acoustics, electromagnetics, thermodynamics. They reflect the properties of conservation and the inverse laws. The Poisson equation is as follows:

$$\nabla^2\phi = -4\pi\rho, \tag{1}$$

where ϕ is normally a potential and ρ is a source or sink density. The equation is known as the Laplace equation when the right-hand side is identical to zero. In general, physical situations governed by these equations are termed as potential problems and represent a very large class of problems in which dissipation is absent.

According to the indirect formulation for the BEM, the expression for the potential (ϕ) at a location ($\vec{r}$) is as follows:

$$\phi(\vec{r}) = \frac{1}{4\pi\varepsilon}\int_V G(\vec{r},\vec{r}')\rho(\vec{r}')\,\mathrm{d}V + \frac{1}{4\pi}\int_{S=\partial V}\left\{G(\vec{r},\vec{r}')\frac{\partial\phi(\vec{r}')}{\partial n'} - \phi(\vec{r}')\frac{\partial G(\vec{r},\vec{r}')}{\partial n'}\right\}\mathrm{d}S', \tag{2}$$

where $\vec{r}$ is the position vector at which the potential is being evaluated, $\vec{r}'$ the location of the distribution density function ρ, V the physical volume and S the surface enclosing the volume, n' is the unit normal vector pointing outward at $\vec{r}'$ and $G(\vec{r},\vec{r}')$ the Green function. In general, the Green function has the form

$$G(\vec{r},\vec{r}') = \frac{1}{|\vec{r}-\vec{r}'|} + F(\vec{r},\vec{r}'), \tag{3}$$

where $F(\vec{r},\vec{r}')$ is a solution of the Laplace's equation

$$\nabla^2 F(\vec{r},\vec{r}') = 0. \tag{4}$$

For electrostatic problems, the BIE reduces to [8]

$$\phi(\vec{r}) = \int_S G(\vec{r},\vec{r}')\rho(\vec{r}')\,\mathrm{d}S', \tag{5}$$

where $\rho(\vec{r}')$ now represents the charge density at $\vec{r}'$, $G(\vec{r},\vec{r}') = 1/4\pi\varepsilon|\vec{r}-\vec{r}'|$ and ε is the permittivity of the medium.

As discussed above, the above equation is normally solved using a collocation technique where the boundary is discretized into a large number of small elements on which the surface charge density is assumed to be constant. The centroid of each element is considered to be the collocation point and the value of the potential there is assumed to represent the potential on the element. Moreover, the distributed charge on the element is assumed to be concentrated at the collocation point except for special cases (e.g., self induction). This severe approximation leads to significant error in the near-field of the elements as will be discussed below.

In order to overcome the limitation of assuming the charge to be concentrated at the collocation points of the boundary elements, we integrated Eq. (5) [9] and obtained analytic expressions which have been incorporated in the present BEM solver. In general, the potential ϕ at a point (X, Y, Z) in free space due to uniform source distributed on a rectangular flat surface having corners situated at $(x_1, 0, z_1)$ and $(x_2, 0, z_2)$ is known to be a multiple of

$$\phi(X,Y,Z) = \int_{z_1}^{z_2}\int_{x_1}^{x_2}\frac{\mathrm{d}x\,\mathrm{d}z}{\sqrt{(X-x)^2+Y^2+(Z-z)^2}}, \tag{6}$$

where the value of the multiple depends upon the strength of the source and other physical considerations. For deducing the above expression, the origin of the coordinate system is assumed to be on the plane of the small element which is assumed to be on the XZ plane as shown in Fig. 1. The denominator within the integral can be easily interpreted to be the distance $\vec{r}$ between the point $P(X, Y, Z)$ at which the potential is being evaluated and an infinitesimal element on the surface situated at $(x, 0, z)$. The closed form expression for $\phi(X, Y, Z)$ is as follows:

$$\begin{aligned}\phi(X,Y,Z) &= \frac{1}{2}\left(2Z\ln\left(\frac{D_2-(X-x_1)}{D_1-(X-x_1)}\right)\right.\\ &\quad + 2Z\ln\left(\frac{D_3-(X-x_2)}{D_4-(X-x_2)}\right)\\ &\quad + 2x_1\ln\left(\frac{D_1-(Z-z_1)}{D_2-(Z-z_2)}\right) + 2x_2\ln\left(\frac{D_4-(Z-z_2)}{D_3-(Z-z_1)}\right)\\ &\quad \left. + 2z_1\ln\left(\frac{D_1-(X-x_1)}{D_3-(X-x_2)}\right) + 2z_2\ln\left(\frac{D_4-(X-x_2)}{D_2-(X-x_1)}\right)\right)\end{aligned}$$

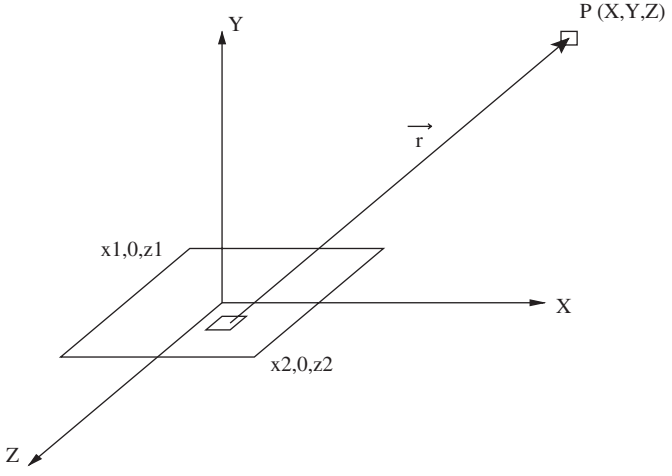

Fig. 1. Geometry of the plates in MEMS.

$$
\begin{aligned}
&- S_1(X + i|Y|)\tanh^{-1}\left(\frac{R_1 - iI_1}{D_1|Z - z_1|}\right)\\
&- S_1(X - i|Y|)\tanh^{-1}\left(\frac{R_1 + iI_1}{D_1|Z - z_1|}\right)\\
&+ S_2(X + i|Y|)\tanh^{-1}\left(\frac{R_2 - iI_1}{D_2|Z - z_2|}\right)\\
&+ S_2(X - i|Y|)\tanh^{-1}\left(\frac{R_2 + iI_1}{D_2|Z - z_2|}\right)\\
&+ S_1(X + i|Y|)\tanh^{-1}\left(\frac{R_1 - iI_2}{D_3|Z - z_1}\right)\\
&+ S_1(X - i|Y|)\tanh^{-1}\left(\frac{R_1 + iI_2}{D_3|Z - z_1|}\right)\\
&- S_2(X + i|Y|)\tanh^{-1}\left(\frac{R_2 - iI_2}{D_4|Z - z_2|}\right)\\
&-S_2(X - i|Y|)\tanh^{-1}\left(\frac{R_2 + iI_2}{D_4|Z - z_2|}\right)\Bigg) - 2\pi Y, \qquad (7)
\end{aligned}
$$

where

$$
\begin{aligned}
&D_1 = \sqrt{(X - x_1)^2 + Y^2 + (Z - z_1)^2},\\
&D_2 = \sqrt{(X - x_1)^2 + Y^2 + (Z - z_2)^2},\\
&D_3 = \sqrt{(X - x_2)^2 + Y^2 + (Z - z_1)^2},\\
&D_4 = \sqrt{(X - x_2)^2 + Y^2 + (Z - z_2)^2},\\
&R_1 = Y^2 + (Z - z_1)^2,\ R_2 = Y^2 + (Z - z_2)^2,\\
&I_1 = (X - x_1)|Y|,\ I_2 = (X - x_2)|Y|,\\
&S_1 = \mathrm{sign}(z_1 - Z),\ S_2 = \mathrm{sign}(z_2 - Z).
\end{aligned}
$$

Similarly, the force field for the above problem is given as a multiple of

$$
\vec{F}(X, Y, Z) = \int_{z_1}^{z_2}\int_{x_1}^{x_2} \frac{\hat{r}\,\mathrm{d}x\,\mathrm{d}z}{r^2}, \qquad (8)
$$

where $\vec{r}$ is the displacement vector from a small surface element to the (X, Y, Z) point where the force field is being evaluated. Eq. (8) has also been integrated in order to get exact expressions to estimate the force fields in the X, Y and Z directions. These expressions, valid for the complete physical domain, are as follows:

$$
\begin{aligned}
F_x(X, Y, Z) = &\ln\left(\frac{D_1 - (Z - z_1)}{D_2 - (Z - z_2)}\right)\\
&- \ln\left(\frac{D_3 - (Z - z_1)}{D_4 - (Z - z_2)}\right), \qquad (9)
\end{aligned}
$$

$$
\begin{aligned}
F_y(X, Y, Z) = &-\frac{1}{2} i\,\mathrm{sign}(Y)\\
&\times \left(S_2\tanh^{-1}\left(\frac{R_2 + iI_2}{D_4|Z - z_2|}\right)\right.\\
&- S_2\tanh^{-1}\left(\frac{R_2 - iI_2}{D_4|Z - z_2|}\right)\\
&+ S_1\tanh^{-1}\left(\frac{R_1 - iI_2}{D_3|Z - z_1|}\right)\\
&- S_1\tanh^{-1}\left(\frac{R_1 + iI_2}{D_3|Z - z_1|}\right)\\
&+ S_2\tanh^{-1}\left(\frac{R_2 - iI_1}{D_2|Z - z_2|}\right)\\
&- S_2\tanh^{-1}\left(\frac{R_2 + iI_1}{D_2|Z - z_2|}\right)\\
&+ S_1\tanh^{-1}\left(\frac{R_1 + iI_1}{D_1|Z - z_1|}\right)\\
&\left.-S_1\tanh^{-1}\left(\frac{R_1 - iI_1}{D_1|Z - z_1|}\right)\right) + C, \qquad (10)
\end{aligned}
$$

$$
\begin{aligned}
F_z(X, Y, Z) = &\ln\left(\frac{D_1 - (X - x_1)}{D_2 - (X - x_1)}\right)\\
&- \ln\left(\frac{D_3 - (X - x_2)}{D_4 - (X - x_2)}\right). \qquad (11)
\end{aligned}
$$

In Eq. (10), C is a constant of integration as follows:

$$
C = \begin{cases} 0 & \text{if outside the extent of the flat surface,}\\ 2\pi & \text{if inside the extent of the surface and } Y > 0,\\ -2\pi & \text{if inside the extent of the surface and } Y < 0. \end{cases}
$$

Eqs. (7) and (9)–(11) are exact and valid throughout the physical domain including the near-field. These are the equations we have used to develop the nearly exact BEM solver as described in the next section. We have also presented the results of numerical experiments carried out to establish the accuracy and effect of these expressions in the first part of results and discussions.

3. Numerical implementation

In BEM, as applied in electrostatics in the absence of any space charges, the charge carrying surfaces (normally the boundaries) of a system are segmented on which unknown uniform charge densities are assumed to be distributed. The unknown uniform charge densities (ρ) and the known voltages (ϕ) at the discrete points are related through the influence matrix (**A**),

$$
\mathbf{A} \cdot \rho = \phi,
$$

where A_{ij} of **A** represents the potential at the midpoint of segment i due to a unit charge density distribution at the segment j. The unknown surface charge densities can then be calculated by inverting the influence coefficient matrix and multiplying it to the potential column vector as follows:

$$
\rho = \mathbf{A}^{-1} \cdot \phi. \qquad (12)
$$

From the charge densities, it is easy to obtain the charge in each of the segments. In this work, we have used the lower–upper (LU) decomposition incorporating Crout's method of partial pivoting to solve for ρ.

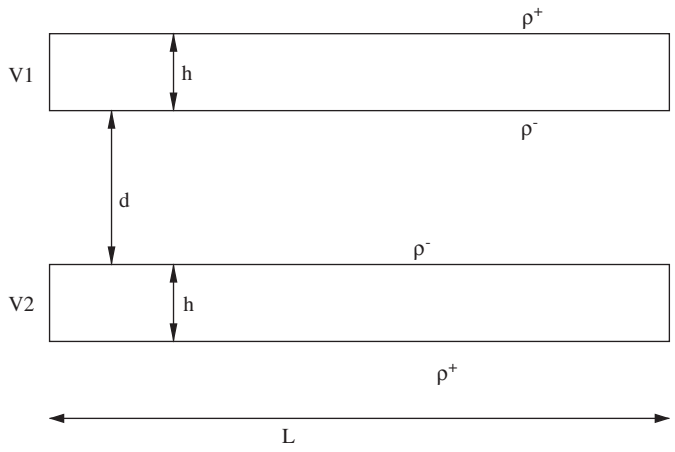

Fig. 2. Geometry of the model parallel plate capacitor.

For the present problem of estimating electrostatic field for plate structures relevant to MEMS, the geometry considered is as shown in Fig. 2. We are interested in the Dirichlet problem for Laplace's equation for this geometry. Because of the peculiarities of MEMS structures, the charge density distributions on the upper and lower surfaces of a plate have to be solved for separately (designated by ρ^+ and ρ^-). So, in all, four or twelve surfaces are discretized, the influence matrix is set up and charge densities at each of the element obtained using Eq. (12). While setting up the influence matrix and also in all subsequent calculations involving potentials and force fields (on the boundary or at any field point), the expressions presented by Eqs. (7) and (9)–(11) have been used.

It is well known that the charge densities near the edges of these bodies are much higher than those far away from the edges. In order to minimize the errors resulting from the approximation of uniform charge density, we have progressively reduced the segment size close to the edges using a simple polynomial expression as used in [5]. Although a true adaptive segmentation is a better approach for these problems, the simple method has improved the results substantially. In fact, it has been suggested [5] that the simple algebraic expressions can actually yield more accurate results since the adaptive approach may lead to variation of segment sizes which is not smooth.

4. Results

4.1. Numerical experiments

In order to establish the accuracy of the above expressions, we have compared the potential and electric field distributions computed using the new expressions with those computed by assuming a varying degree of discretization of the given surface, where each of the discrete elements is assumed to have its charge concentrated at its centroid. The flat surface has been assumed to be a square (1 cm × 1 cm) and length scales up to 10 μm have been resolved. The source density on the flat surface has been assumed to be of unit strength. In the Figs. 3 and 4, we have presented a comparison among results obtained by the exact expressions and those obtained by discretizing the flat surface having a single element, having 10×10 elements and having 100×100 elements. The single element representation gives inaccurate results as soon as the point is less than 1 cm away from the origin. The 10×10 discretization is satisfactory only up to the edge of the surface (i.e., 5 mm away from the origin), while the 100×100 discretization yields good results close to origin. The last one, however, shows fine oscillations when inspected closely. In order to illustrate the error incurred through the use of point singularity rather than a distributed one, we have plotted the deviation from the exact value depending on the amount of discretization used. The deviation normalized with respect to the exact value of the potential has been plotted as a function of distance along X and Y axes, as shown in Fig. 5 and 6. In order to accommodate the large variation of magnitude of the error, a logarithmic scale has been used. It can be seen that the usual boundary element approximation leads to a very large amount of error (more than 10%) as potentials at points on the element are evaluated. The error increases as we move towards the centroid of the element. At the centroid, however, the point approximation leads to a singularity and, in its place, an exact analytic expression is normally used which gives correct result. With further subdivision, the accuracy increases but at the cost of a large increase in computational expenses. For example, with a 10×10 subdivision, the error within the element drops to around 5%. The error is less than 1% only if the influencing element is subdivided into approximately 100×100

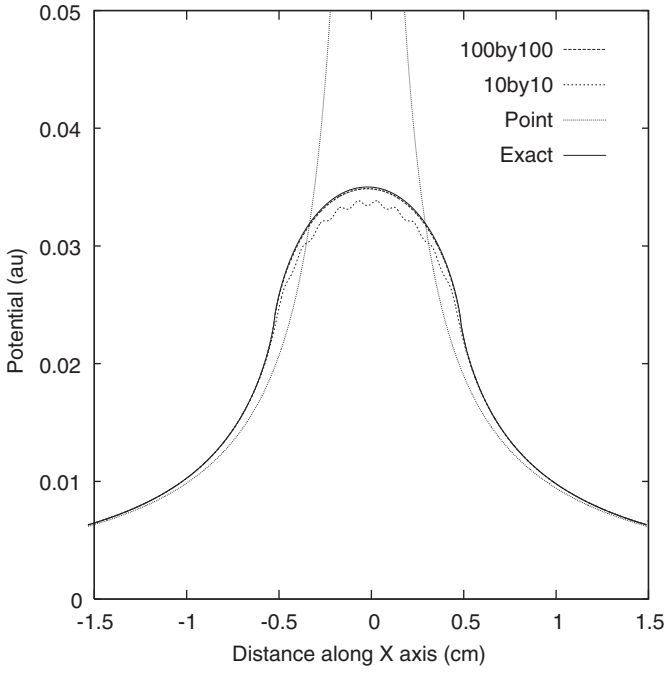

Fig. 3. Comparison of potential distribution along X-axis.

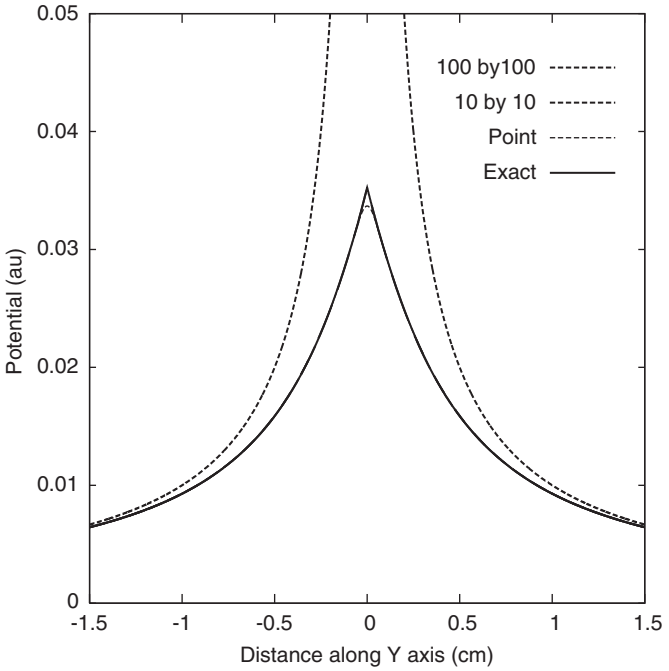

Fig. 4. Comparison of potential distribution along Y-axis.

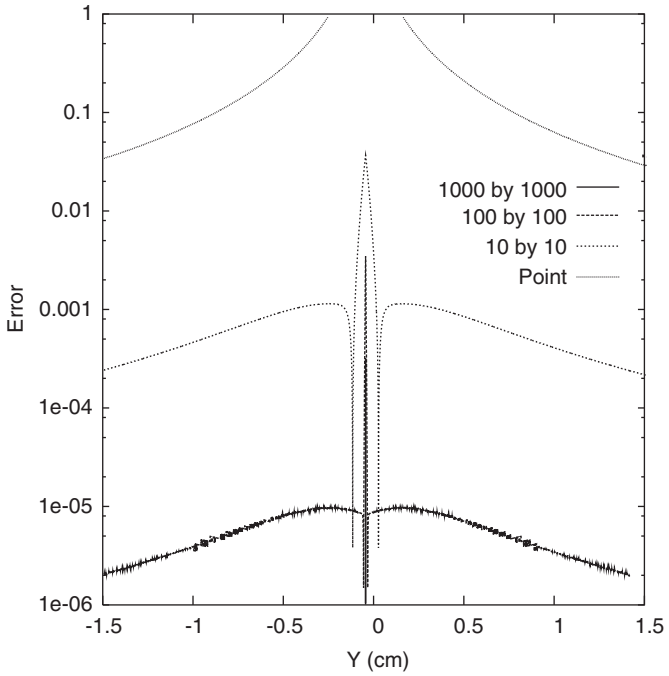

Fig. 6. Variation of error along Y-axis.

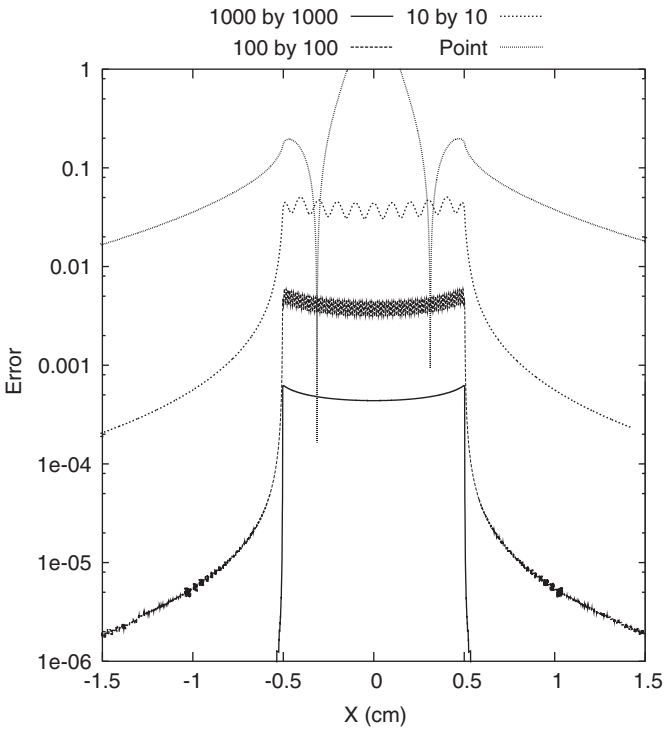

Fig. 5. Variation of error along X-axis.

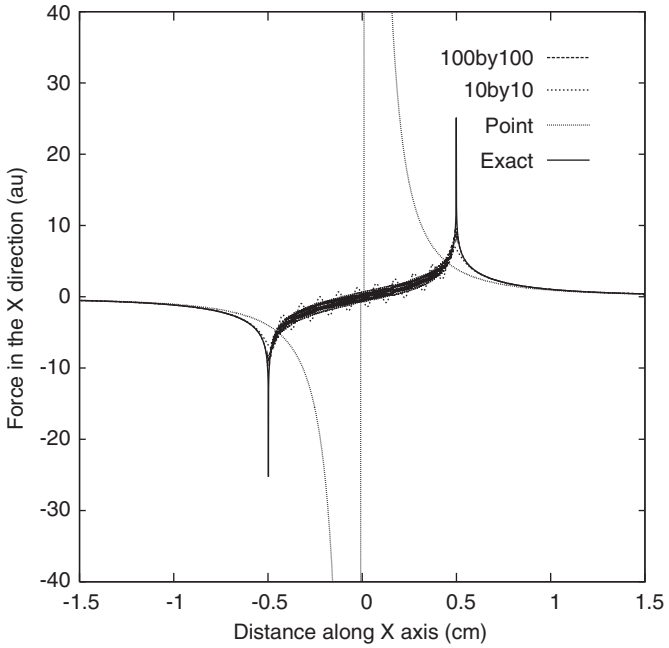

Fig. 7. Comparison of F_x distribution along X-axis.

elements which involves a very large computational expense indeed. It may be noted here that for the standard approximation, the error along the X-axis drops below 1% only after the distance from the centroid is more than twice the length of the element. A similar analysis of the error along the Y-axis indicates that the error drops below 1% beyond three times the length of the element. So, in general, the standard BEM approximation can be assumed to yield accurate results only if the distance of the influenced point from the centroid of the influencing element is more than three times the length of the element.

Similarly, Figs. 7 and 8 show the comparison of force values computed using the exact expression, the standard BEM approximation and computations using a segmented

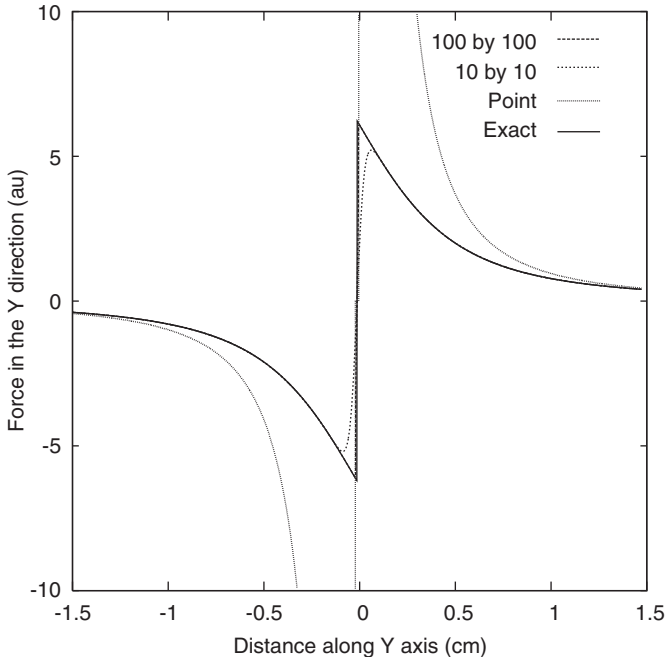

Fig. 8. Comparison of F_y distribution along Y-axis.

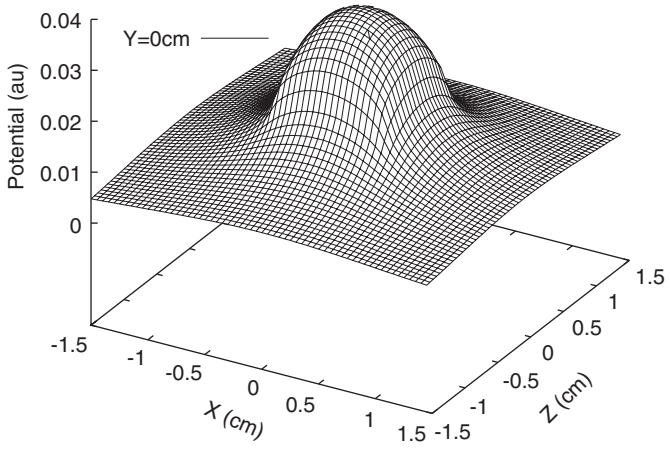

Fig. 9. Potential surface distribution on the flat surface.

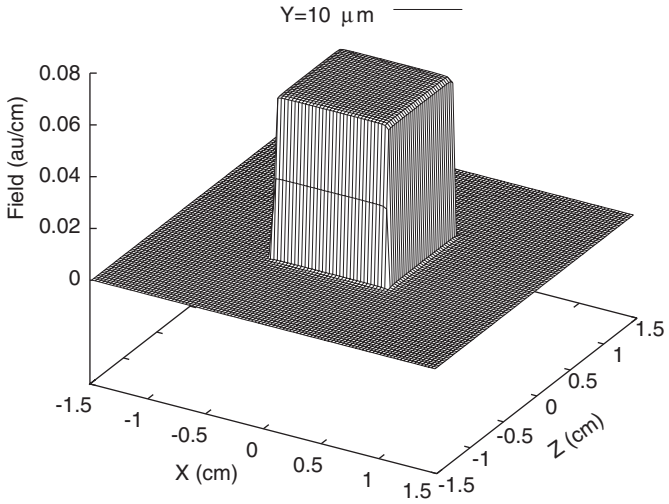

Fig. 10. F_y surface distribution at $Y = 10\,\mu m$.

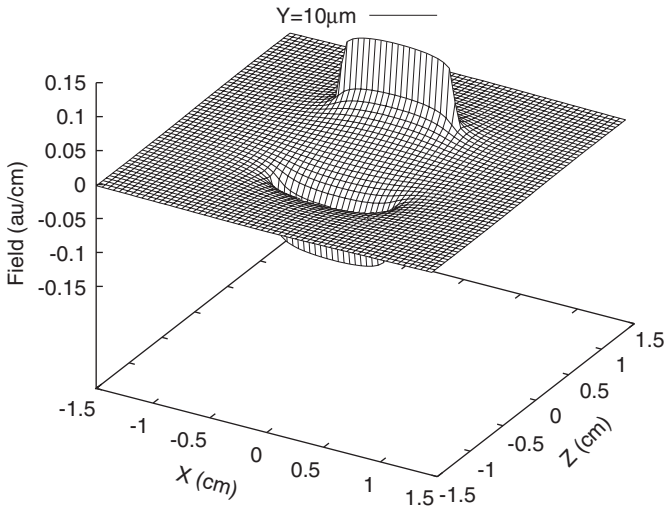

Fig. 11. F_z surface distribution at $Y = 10\,\mu m$.

element. It can be seen that for F_x (Fig. 7), even the highest discretization (100×100) leads to significant amount of oscillation in the estimate while the exact expressions yield a force varying smoothly along the X-axis. It is well known that for the charged surface considered, there should be a 'jump' in F_y from $+2\pi$ to -2π at the centroid, as we move from positive Y to negative values. From Fig. 8, it is clear that this 'jump' is accurately computed by Eq. (10).

In Figs. 9–11 we have presented the surface plots of the potential, force in the Y direction and force in the Z direction in the near-field region. The potential surface has been drawn on the element surface while the force fields have been drawn just 10 μm away from the surface. While the far-field potential and force surfaces mimic the behavior due to a point source, these near-field surface plots are found to be markedly different. The figures vividly represent the error incurred in modeling distributed sources using the point approximation.

From all these figures, we can conclude that the exact expressions reproduce the correct features of the fields within the near-field even in the most difficult situations, e.g., where there is jump in the value (Fig. 8), or where there are sharp discontinuities (Figs. 4 and 7).

4.2. Parallel plate capacitive structures relevant to MEMS

A parallel plate capacitor with two square plates as shown in Fig. 2 has been considered as the model problem for structures used in MEMS. The length L has been considered to be unity while different values of h, the thickness of each plate, and d, the distance between the two facing surfaces of the two plates, have been considered. The medium external to the plates has been considered to be vacuum. The potential applied to the upper and lower

plates are $V_1 = 1$ and $V_2 = -1$, respectively. Similar capacitive structures have been considered by [6,10]. In the former, a special BIE formulation was developed to treat plates of medium thickness (enhanced BEM) and another to treat thin plates (thin plate BEM). Our attempt here will be to compare the results obtained using the nearly exact BEM solver with those obtained using these special formulations for capacitive structures of a wide range of d and h. It may be noted here that capacitance (C) has been computed as $C = Q/2V$ where Q is the total charge on the upper plate while V is the potential on it. The value of the capacitance has been normalized using the conventional formula $Cd/A\varepsilon$ where A is the area of the upper plate.

In Table 1, we have presented the variation of the normalized capacitance for $d/L = 0.2$ with h/L varying from 1 to 10^{-6}. The present results have been compared with those in [6] obtained using the usual BEM, enhanced BEM and thin plate BEM formulations. It can be seen that there is a good amount of discrepancy in the values of the normalized capacitance. Here it must be remembered that while the usual BEM is not expected to produce correct results for thin plates, the enhanced BEM is also not expected to yield accurate results for the whole range of h/L. Similarly, the thin plate BEM is expected to give correct results only when $h/L \leqslant 0.001$. One important point to note is that while the thin plate BEM indicates an increase in the normalized capacitance with the decrease in h/L, the present results, as well as the enhanced BEM results, indicate an opposite dependence. This is possibly because of the reason that the thin-plate formulation does not incorporate the effect of the sides of the plate in an explicit manner. This thickness, h, is likely to have a negligible effect on the total charge accumulated on the plate only when it is extremely small. Since, for plates with $h/L \geqslant 0.001$, this cannot be expected to hold true, it is safe not to use the thin-plate formulation for these plates. In order to illustrate this behavior, we have presented the value of normalized capacitance computed by the presented solver in the fifth column of Table 1 for which the total charge accumulated on the plate has been assumed to be only due to the upper and lower surfaces of the plate. It can be observed that the values in this column are quite close to those computed by the thin-plate BEM and follow the same trend. The last column of Table 1 contains the correct values of normalized capacitance as calculated by the solver based up on the proposed expressions. Here, the contribution of all the sides of a plate are considered when computing the total charge accumulated on the plate. As expected, the obtained value for normalized capacitance agrees with the usual BEM value when $h/L = 1$, follows the trend of the enhanced BEM for intermediate values of h/L and agrees reasonably well with the thin plate BEM when $h/L \leqslant 0.001$. Thus, using the same formulation, expressions and solver, it has been possible for us to obtain accurate values of the normalized capacitance for the whole range of h/L. It may be mentioned here that the value of normalized capacitance in the fifth and sixth columns of the table tend to converge for smaller values of h/L, justifying the thin plate BEM formulation and also demonstrating the accuracy of the present formulation.

In Fig. 12, we present the variation of the normalized capacitance of a system with $h/L = 10^{-6}$ and changing d. From the rather small value of h/L it is expected that this case corresponds to thin plate capacitors which are often used as components of MEMS structures. Our results have been compared with those from [6,10]. It can be seen that the present results fall in between those of the other two, being almost identical to the thin plate BEM results of [6]. The close match between the results confirms that the new solver does not require any special formulation to handle the most stringent of geometrical constraints. In this case the proximity of the two surfaces of the plates under consideration would have led to sure failure of any usual BEM solver (and also the enhanced BEM solver as shown in [6]).

In Fig. 13, we present the charge density on the upper and lower surfaces of the upper plate of Fig. 2 and compare our values with those from [6]. In this case, the $h/L = 10^{-3}$ while $d/L = 0.2$. The values are in excellent agreement throughout most of the span. However, we have not found any 'bump' towards the end of the plate. In fact, such bumps could be observed only when we used very coarse discretization and is probably an artifact, as has been remarked in [6]. The fact that the new solver computes charge density without the 'bumps' has led us to believe

Table 1
Variation of normalized capacitance for $d/L = 0.2$ with varying h/L

h/L	Usual BEM [6]	Enhanced BEM [6]	Thin plate BEM [6]	Present (excluding side)	Present (including side)
1.0	2.3975			1.259038	2.374961
0.1	3.3542	2.6631	1.2351	1.360813	1.757175
0.05		1.7405	1.3879	1.392805	1.679710
0.01		1.6899	1.5611	1.455047	1.590639
0.005		1.6652	1.5874	1.475206	1.574417
0.001		1.6221	1.6094	1.511291	1.558108
0.000001			1.6200 (1.5830 with finer mesh)	1.539550	1.552190

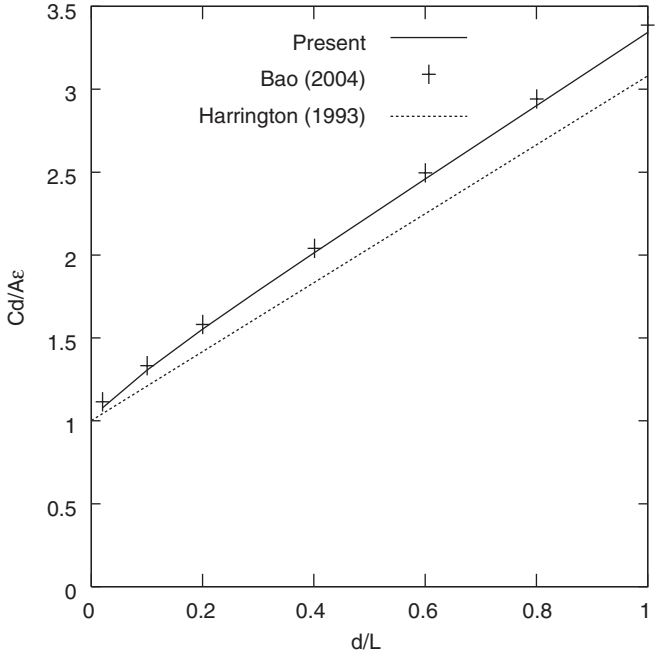

Fig. 12. Variation of normalized capacitance with varying d.

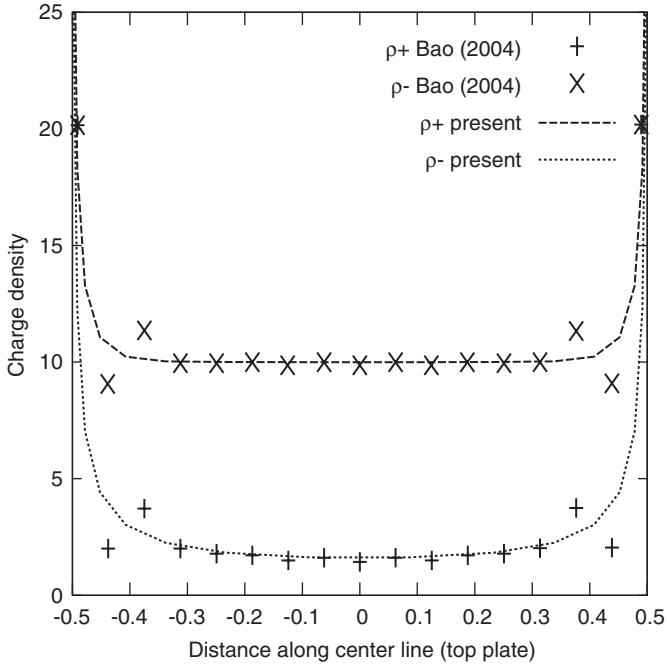

Fig. 13. Comparison of charge density on the top plate.

that the present results are more accurate than those available. It seems that the small disagreement in the earlier comparison of normalized capacitance (Fig. 12) stems from these artifacts present in the surface charge density computation of [6].

In Table 2, we have presented a comparison of the surface charge density computed by various methods. The enhanced BEM method is found to overestimate the value of the surface charge density for $h/L = 0.001$. For the thicker plate its estimates are similar to the thin plate BEM and the present results.

Finally, in Table 3, we present a study on how the accuracy of the results obtained using the presented solver depends on the amount of discretization. The discretization has been varied on the top and bottom surfaces of the plates only, while the same discretization has been maintained for the side surfaces (10×4 on each side for plates having $h/L \leqslant 0.001$ and 10×10 for plates having h/L greater than that). It can be seen that the values computed for all the discretizations are similar and fairly accurate results are obtained with even the coarsest 10×10 discretization. It may be mentioned here that number of elements in this case is 720 for thin plates which is reasonably small. For the most accurate computation (30×30 discretization), the number of elements is 3920. This computation also, although time consuming, can be easily undertaken on a present day desktop computer. The discretization of 20×20 for the top and bottom surfaces of a plate seems to yield accurate results without requiring long computation time. In this case, the number of elements turn out to be 1920. Please note that the assumption of symmetry has not been implemented for any of the results presented in this work. A suitable implementation can drastically reduce the amount of computation.

The present formulation is based on rectangular elements which are known to create problems while modeling generalized three-dimensional objects. Hence, in order to make the presented approach more versatile, we have started to work on developing a similar formulation based on triangular elements so that the solver can be extended to model geometries that require unstructured mesh.

5. Conclusions

Exact expressions for potential and force field due to a uniform source distribution on a flat surface have been

Table 2
Comparison of surface charge density values for $d/L = 0.2$

Method	Enhanced BEM [6]	Thin plate BEM [6]	Present	Enhanced BEM [6]	Thin plate BEM [6]	Present
h/L	0.01	0.01	0.01	0.001	0.001	0.001
ρ^+ at plate center	1.9972	1.4539	1.6008	4.5300	1.4500	1.6264
ρ^- at plate center	9.8761	9.4399	9.9983	12.150	9.8600	9.9988

Table 3
Variation of accuracy with discretization for $d/L = 0.2$ for different h/L

h/L	Mesh on top and bottom	Mesh on sides	Normalized BEM capacitance
0.1	10×10	10×10	1.756467
	20×20	10×10	1.757175
	30×30	10×10	1.757083
0.01	10×10	10×10	1.588973
	20×20	10×10	1.590639
	30×30	10×10	1.590558
0.001	10×10	4×10	1.55591
	20×20	4×10	1.558108
	30×30	4×10	1.558268
0.000001	10×10	4×10	1.548260
	20×20	4×10	1.552190
	30×30	4×10	1.552516

presented. The expressions have been found to yield very accurate results in the complete physical domain. Of special importance is their ability to reproduce the complicated field structure in the near-field region. The errors inducted in assuming discrete point sources to represent a continuous distribution have been illustrated. The use of the new expressions in a BEM solver can help in relaxing the most damaging of approximations involved in the development of the solver.

A BEM solver has been developed based on the exact expressions for potential and force fields. The nearly exact solver has been used to compute the electrostatic properties of structures relevant to MEMS. The obtained results have been compared with other available results. The comparison indicates that the presented ones are possibly more accurate than the available results. Thus, it may be said that the new solver yields precise results for a very wide range of electrostatic configuration without needing special formulations for critical geometries. The presented approach can be equally helpful for several other areas of science and technology that are governed by similar mathematics.

Acknowledgments

We would like to thank Professor Bikash Sinha, Director, SINP and Professor Sudeb Bhattacharya, Head, NAP Division, SINP for their encouragement and support throughout the work.

References

[1] Cheng AH-D, Cheng DT. Heritage and early history of the boundary element method. Eng Analysis Boun Elem 2005;29:268–302.
[2] Mukhopadhyay S, Majumdar N. Effect of finite dimensions on the electric field configuration of cylindrical proportional counters. IEEE Trans Nucl Sci 2006;53 (to be published).
[3] Renau A, Read FH, Brunt JNH. The charge-density method of solving electrostatic problems with and without the inclusion of space-charge. J Phys E: Sc Instrum 1982;15:347–54.
[4] Goto E, Shi Y, Yoshida N. Extrapolated surface charge method for capacity calculation of polygons and polyhedra. J Comput Phys 1992;100:105–15.
[5] Read FH. Improved extrapolation technique in the boundary element method to find the capacitances of the unit square and cube. J Comput Phys 1997;133:1–5.
[6] Bao Z, Mukherjee S. Electrostatic BEM for MEMS with thin conducting plates and shells. Eng Analysis Boun Elem 2004; 28:1427–35.
[7] Senturia SD, Harris RM, Johnson BP, Kim S, Nabors K, Shulman MA, White JK. A computer-aided design system for microelectromechanical systems (MEMCAD). J Micro Electro Mech Syst 1992;1:3–13.
[8] Shi F, Ramesh P, Mukherjee S. On the application of 2D potential theory to electrostatic simulation. Commun Numer Meth Engng 1995;11:691–701.
[9] Etter DM. Engineering problem solving with matlab. 2nd ed. Englewood Cliffs, NJ: Prentice-Hall; 1993.
[10] Harrington RF. Field computation by moment methods. Piscataway, NJ: IEEE Press; 1993.